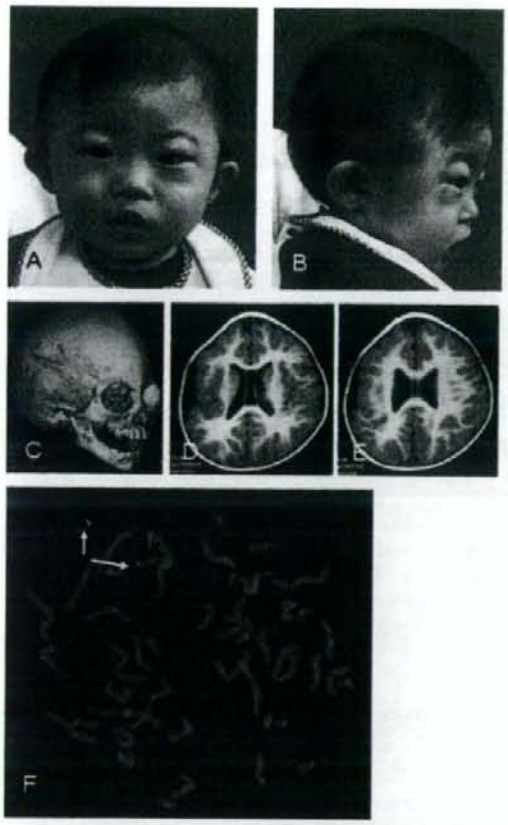

FIG. 1. The patient at age 18 months (**A**, **B**). Three-dimensional computed tomography of the skull, showing synostosis of the metopic suture (**C**). Brain magnetic resonance imaging, showing polymicrogyria of the right hemisphere (**D**, **E**). FISH analysis of the patient using TUPLE1 SpectrumOrange at 22q11.2 (red arrowhead) and ARSA SpectrumGreen Control Probe at 22q13.3 (green arrows) (**F**). [Color figure can be viewed in the online issue, which is available at www.interscience.wiley.com.]

eyelids, a low nasal bridge, hypoplastic nasal alae, low-set lop ears, a small mouth, high-arched palate, and micrognathia (Fig. 1A,B). At age 11 months, his OFC was 43 cm (−2.1 SD). When he moved his right hand, his left hand moved in a mirror fashion. A neurological examination showed left hemifacial palsy, left hemiplegia, and left ankle clonus. Radiography demonstrated complete synostosis of the metopic suture (Fig. 1C). Brain MRI showed polymicrogyria of the right hemisphere (Fig. 1D,E). Linear craniectomy of the metopic suture was performed at age 18 months. At age 2 years, he walked with support, and spoke few words. He had febrile convulsions, and his EEG showed spike activities in the right fronto-central region. Sequencing analysis of the fibroblast growth factor receptor 2 (*FGFR2*) gene detected no mutation [Yamamoto et al., 2001].

TABLE I. FISH Analysis of the 22q11.21-11.22 Region

Probe	Band	Distance from 22pter (Mb)	Patient	Father	Mother
RP11-100K2	22q11.21	16.8	+	+	
TUPLE 1	22q11.21	17.7	−	−	+
RP11-165F18	22q11.21	19.6	−	−	
RP11-36N5	22q11.21	20.3	+	+	
RP11-757F24	22q11.22	21.1	+	+	

−, absent FISH signal; +, presence of the signal.

The mother was healthy and phenotypically normal. The father was of normal intelligence but had the facial gestalt characteristic of an adult with the deletion 22q11.2 syndrome, including long face, narrow palpebral fissures, square root of the nose, hypoplastic nasal alae, and small mouth. His speech was nasal.

CYTOGENETIC STUDIES

G-banded chromosomes of the boy were 46,XY. Fluorescent in situ hybridization (FISH) analysis using LSI DiGeorge/VCFS Region Probe (Vysis, Inc., Downers Grove, IL) detected a deletion in the patient and the father, but not in the mother (Fig. 1F). FISH using probes spanning the 22q11.21-11.22 region detected a 3-Mb deletion in both the father and son (Table I).

DISCUSSION

The present patient and the father showed the typical gestalt of conotruncal anomaly face syndrome, including a narrow nose with its squared root and narrow ala nasi, and short palpebral fissures [Matsuoka et al., 1994]. These and additional clinical manifestations identified in the patient, including mental and motor developmental delay, microcephaly, seizures, polymicrogyria, and cardiac anomalies were clues for the identification of 3-Mb deletion of 22q11.2 region in this family. This clinical variability from full manifestation to extremely mild clinical anomalies in familial deletion 22q11.2 as seen in this family is a well-known phenomenon [Digilio et al., 2003]. Hemicephalic polymicrogyria revealed in the patient is also a well-known rare complication of deletion 22q11.2 syndrome [Sztriha et al., 2004], but the exception is trigonocephaly.

Trigonocephaly is seen in some chromosomal abnormalities such as monosomy 9p and partial monosomy 11q, as well as in other genetic disorders [Azimi et al., 2003; Jehee et al., 2005; Yatsenko et al., 2005]; a candidate region for monosomy 9p syndrome had recently been narrowed by our group [Kawara et al., 2006]. However, deletion 22q11.2 syndrome has never been listed as the cause of trigonocephaly. Ryan et al. [1997] summarized a

spectrum of clinical features of deletion 22q11.2 syndrome, and described five patients with craniosynostosis without descriptions of its type. McDonald-McGinn et al. [2005] reported four patients with deletion 22q11.2 syndrome associated with craniosynostosis, all of whom showed synostosis of the coronal suture but not involving the metopic suture. Therefore, the present report is the first description of a relationship between deletion 22q11.2 syndrome and trigonocephaly.

Although the exact cause of the coexistence of deletion 22q11.2 and trigonocephaly remains unknown, and coincidental occurrence might be the explanation for this. Alternatively, symptoms of trigonocephaly might be a minor complication of deletion 22q11.2. Another possibility, but less likely, is a mutated trigonocephaly gene mapped to 22q11.2 and derived from the mother was unmasked by the deletion in the patient.

ACKNOWLEDGMENTS

This study was funded by the Japan Society for the Promotion of Science to T.Y. and SORST from Japan Science and Technology Agency to N.M. and K.N.

REFERENCES

Azimi C, Kennedy SJ, Chitayat D, Chakraborty P, Clarke JT, Forrest C, Teebi AS. 2003. Clinical and genetic aspects of trigonocephaly: A study of 25 cases. Am J Med Genet Part A 117A:127–135.

Digilio MC, Angioni A, De Santis M, Lombardo A, Giannotti A, Dallapiccola B, Marino B. 2003. Spectrum of clinical variability in familial deletion 22q11.2: From full manifestation to extremely mild clinical anomalies. Clin Genet 63:308–313.

Emanuel BS, McDonald-McGinn D, Saitta SC, Zackai EH. 2001. The 22q11.2 deletion syndrome. Adv Pediatr 48:39–73.

Jehee FS, Johnson D, Alonso LG, Cavalcanti DP, de Sa Moreira E, Alberto FL, Kok F, Kim C, Wall SA, Jabs EW, Boyadjiev SA, Wilkie AO, Passos-Bueno MR. 2005. Molecular screening for microdeletions at 9p22-p24 and 11q23-q24 in a large cohort of patients with trigonocephaly. Clin Genet 67:503–510.

Kawara H, Yamamoto T, Harada N, Yoshiura K, Niikawa N, Nishimura A, Mizuguchi T, Matsumoto N. 2006. Narrowing candidate region for monosomy 9p syndrome to a 4.7-Mb segment at 9p22.2-p23. Am J Med Genet Part A 140A:373–377.

Matsuoka R, Takao A, Kimura M, Imamura S, Kondo C, Joh-o K, Ikeda K, Nishibatake M, Ando M, Momma K. 1994. Confirmation that the conotruncal anomaly face syndrome is associated with a deletion within 22q11.2. Am J Med Genet 53:285–289.

McDonald-McGinn DM, Gripp KW, Kirschner RE, Maisenbacher MK, Hustead V, Schauer GM, Keppler-Noreuil KM, Ciprero KL, Pasquariello P Jr, LaRossa D, Bartlett SP, Whitaker LA, Zackai EH. 2005. Craniosynostosis: Another feature of the 22q11.2 deletion syndrome. Am J Med Genet Part A 136A:358–362.

Ryan AK, Goodship JA, Wilson DI, Philip N, Levy A, Seidel H, Schuffenhauer S, Oechsler H, Belohradsky B, Prieur M, Aurias A, Raymond FL, Clayton-Smith J, Hatchwell E, McKeown C, Beemer FA, Dallapiccola B, Novelli G, Hurst JA, Ignatius J, Green AJ, Winter RM, Brueton L, Brondum-Nielsen K, Stewart F, Van Essen T, Patton M, Paterson J, Scambler PJ. 1997. Spectrum of clinical features associated with interstitial chromosome 22q11 deletions: A European collaborative study. J Med Genet 34:798–804.

Spiteri E, Babcock M, Kashork CD, Wakui K, Gogineni S, Lewis DA, Williams KM, Minoshima S, Sasaki T, Shimizu N, Potocki L, Pulijaal V, Shanske A, Shaffer LG, Morrow BE. 2003. Frequent translocations occur between low copy repeats on chromosome 22q11.2 (LCR22s) and telomeric bands of partner chromosomes. Hum Mol Genet 12:1823–1837.

Sztriha L, Guerrini R, Harding B, Stewart F, Chelloug N, Johansen JG. 2004. Clinical, MRI, and pathological features of polymicrogyria in chromosome 22q11 deletion syndrome. Am J Med Genet Part A 127A:313–317.

Yamamoto T, Pipo J, Ninomiya H, Ieshima A, Koeda T. 2001. Antley-Bixler syndrome and maternal virilization: A proposal of genetic heterogeneity. Clin Genet 59:451–453.

Yatsenko SA, Cheung SW, Scott DA, Nowaczyk MJ, Tarnopolsky M, Naidu S, Bibat G, Patel A, Leroy JG, Scaglia F, Stankiewicz P, Lupski JR. 2005. Deletion 9q34.3 syndrome: Genotype-phenotype correlations and an extended deletion in a patient with features of Opitz C trigonocephaly. J Med Genet 42:328–335.

American Journal of Medical Genetics Part A 140A:1737–1743 (2006)

Origin and Mechanisms of Formation of Fetus-in-Fetu: Two Cases With Genotype and Methylation Analyses

Shoko Miura,[1,2,8] Kiyonori Miura,[1]* Toshiyuki Yamamoto,[3] Michiko Yamanaka,[4] Keisuke Saito,[4] Tomoo Hirabuki,[4] Kenji Kurosawa,[5] Naoki Harada,[7,8] Yoko Ishizaki-Yamasaki,[1,2,8] Naomichi Matsumoto,[5,8] Fumiki Hirahara,[6] Koh-ichiro Yoshiura,[2,8] Hideaki Masuzaki,[1] and Norio Niikawa[2,8]

[1]Department of Obstetrics and Gynecology, Nagasaki University Graduate School of Biomedical Sciences, Nagasaki, Japan
[2]Department of Human Genetics, Nagasaki University Graduate School of Biomedical Sciences, Nagasaki, Japan
[3]Division of Medical Genetics, Kanagawa Children's Medical Center, Yokohama, Japan
[4]Division of Obstetrics, Kanagawa Children's Medical Center, Yokohama, Japan
[5]Department of Human Genetics, Yokohama City University Graduate School of Medicine, Yokohama, Japan
[6]Department of Obstetrics, Gynecology and Reproductive Science, Yokohama City University Graduate School of Medicine, Yokohama, Japan
[7]Kyushu Medical Science, Nagasaki, Japan
[8]Solution Oriented Research of Science and Technology (SORST), Japan Science and Technology Agency (JST), Kawaguchi, Japan

Received 1 May 2006; Accepted 20 May 2006

Fetus-in-fetu (FIF) is a condition in which a host infant has a fetus-like mass(es) within its body. We describe here results of molecular genetic analysis in two cases of FIF. In FIF-1, a male host had two retroperitoneal fetiform masses each with a vertebral column, and in FIF-2, a fetiform mass with vertebral column was present in the cranial cavity of a male host. Genotyping of each case using microsatellite markers showed that the host infant and its fetus(es) inherited one copy each of parental alleles and shared identical genotypes. These findings were confirmed by single nucleotide polymorphism (SNP) analysis using Affymetrix GeneChip Human Mapping 50K Array, and supported a monozygotic twin theory of FIF. Analysis of the methylation status was done in both cases at the differentially methylated region (*DMR*) within the human *IGF2-H19* locus after bisulfite treatment, methylation-specific PCR, and cloning of PCR products. Normally, only the paternal allele is methylated and the maternal allele unmethylated in *DMR*. However, in FIF-1, 7 (46.7%) of 15 clones from a fetiform mass and 6 (66.7%) of 9 clones from the other mass showed an unmethylated paternal allele, while the methylation status of a host infant and its fetiform mass in FIF-2 was the same in all clones examined with normal patterns. These data suggest that in FIF-1, two isolated blastocysts originated from one zygote, one of the two was implanted into (or included by) the other blastocyst during the process of methylation, and such abnormal implantation may have occurred in FIF-2 after the establishment of methylation. This is the first case of FIF showing different methylation patterns between a host infant and fetiform mass. © 2006 Wiley-Liss, Inc.

Key words: fetus-in-fetu; genotype; methylation status; origin; mechanism of formation

How to cite this article: Miura S, Miura K, Yamamoto T, Yamanaka M, Saito K, Hirabuki T, Kurosawa K, Harada N, Ishizaki-Yamasaki Y, Matsumoto N, Hirahara F, Yoshiura K, Masuzaki H, Niikawa N. 2006. Origin and mechanisms of formation of fetus-in-fetu: Two cases with genotype and methylation analyses. Am J Med Genet Part A 140A:1737–1743.

INTRODUCTION

A Fetus-in-fetu (FIF) anomaly is a condition of fetiform mass(es) located within a host infant, like a Russian doll "matreshka." The incidence is estimated to be 1/500,000 births [Hoeffel et al., 2000]. Its mechanism of formation has remained unknown. Willis [1935] tried to distinguish it from teratoma by the presence of signs of axiation, metameric segmentation, delamination of germ layers, and organs

Grant sponsor: Ministry of Education, Sports, Culture, Science and Technology of Japan; Grant numbers: 16591670, 17591748, 17019055; Grant sponsor: Japan Science and Technology Agency.

*Correspondence to: Dr. Kiyonori Miura, Department of Obstetrics and Gynecology, Nagasaki University Graduate School of Biomedical Sciences, Sakamoto 1-7-1, Nagasaki 852-8501, Japan.
E-mail: kiyonori@nagasaki-u.ac.jp

DOI 10.1002/ajmg.a.31362

or somatic regions. These characteristics, as well as the presence of the vertebral column, segmental axis or high development of organogenesis, are widely used as definition of FIF [Hoeffel et al., 2000; Brand et al., 2004]. However, the distinction from highly differentiated teratoma maybe difficult [Hoeffel et al., 2000], for example, in the case of highly differentiated limbs or digits without the vertebral column [Eng et al., 1989; Ouimet and Russo, 1989; Naudin ten Cate et al., 1995]. There are two hypotheses on the formation of FIF. The monozygotic twin theory tries to explain FIF by inclusion of sister embryos that arise by an unequal division of the inner cell mass or anastomosis of the vitelline circulation between diamniotic monochorionic twins [Lord, 1956], whereas a highly differentiated teratoma theory is mainly based on the occasional presence of infants with both FIF and teratoma [Heifetz et al., 1988; Gilbert-Barness et al., 2003]. Alternatively, FIF and teratoma may share a causal/pathogenetic mechanism [Higgins and Coley, 2006]. Studies of genetic markers, such as a blood group, sex chromosome constitution, protein polymorphisms, and DNA markers [Hing et al., 1993; Chen et al., 1997; Kumar et al., 1999; Gilbert-Barness et al., 2003; Brand et al., 2004; Higgins and Coley, 2006], suggested that host infants and their fetiform mass are genetically identical.

We recently encountered two cases of FIF. Here we report the results of molecular genetic studies on their origin and methylation status. Possible mechanisms of formation will be discussed.

MATERIALS AND METHODS

FIF-1

A 31-year-old primigravid woman was referred to Kanagawa Children's Medical Center (KCMC) at 25 weeks of gestation for ultrasonographic diagnosis of a fetal abdominal mass. Ultrasonopgraphy (US) at 26 weeks indicated that a 43-mm retroperitoneal cystic mass contained solid tissues. Magnetic resonance imaging (MRI) at 35 weeks suggested a 90-mm irregularly shaped soft tissue mass consisting of shaft-like bones and spinal column (Fig. 1a). US at 37 weeks showed a retroperitoneal cystic mass containing a long bone-like tissue (Fig. 1b). Based on these findings, FIF was the most likely diagnosis. At 38 weeks, a cesarean section was performed, and a male newborn infant weighing 4,026 g was delivered with Apgar scores of 8 at 1 and 5 min. Retroperitoneal

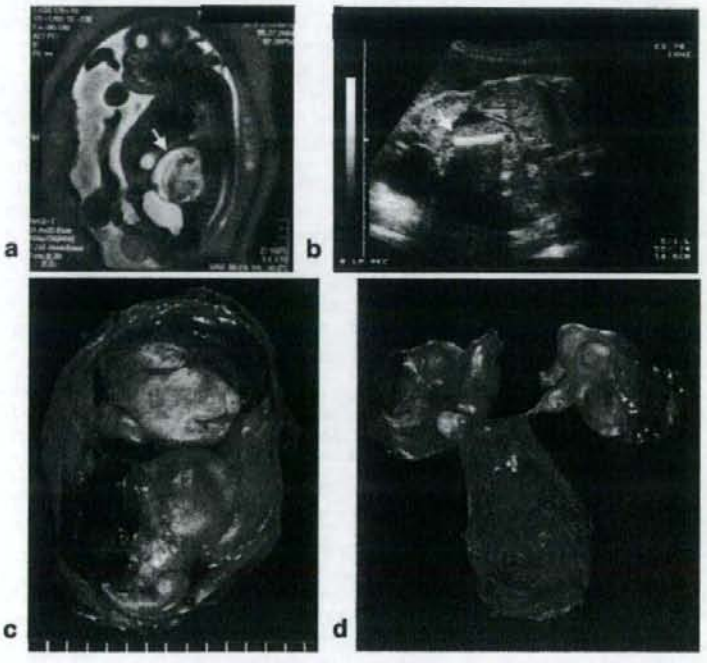

FIG. 1. FIF-1. **a**: Magnetic resonance imaging at 35 weeks showing a vertebral column (arrow). **b**: Ultrasonography (US) at 37 gestational weeks showing a retroperitoneal cystic mass containing a long bone-like structure (arrow). **c** and **d**: A cystic mass covered with a membrane containing two separate fetus-like bodies each with an umbilical cord connected to the host infant's aorta. [Color figure can be viewed in the online issue, which is available at www.interscience.wiley.com.]

tumorectomy, together with left adrenalectomy, was conducted at age 1 day. The cystic mass ($9 \times 9 \times 5$ cm) covered with an amnion-like membrane contained two separate fetiform masses, both almost totally covered with skin and having umbilical cords connected with the host aorta, and also containing oral cavity, limbs, spinal columns (one column was bifid), bowel, thymus, thyroid gland, testis, and other tissues (Fig. 1c, d). There was no placenta-like tissue. Both masses (F-1a and F-1b) were diagnosed as FIF.

FIF-2

A 31-year-old woman was referred to KCMC because of a US pattern of fetal hydrocephaly at 19 weeks of gestation (Fig. 2a). US demonstrated a large fetal head with a diameter of 82 mm (corresponding to the size for a 33-week-old fetus), multiple, high-density, intracranial calcifications, and a 60-mm intracranial tumor. Pregnancy was terminated at 21 weeks of gestation. A male fetus weighing 985 g was delivered. Autopsy showed an intracranial fetiform mass composed of limbs, vertebral column, lung, liver, adrenal, and bowel-like tissues (Fig. 2b), in addition to six irregular, fetiform tumors (Fig. 2c), thus, the largest fetiform mass (F-2) was diagnosed as FIF.

Genotyping at Microsatellite Marker Loci

Whole blood samples were obtained from Hosts 1 and 2 and from their respective parents. Fibroblast cultures were established from both host infants and three fetuses (F-1a, F-1b, and F-2). Genomic DNA was extracted from lymphocytes and fibroblasts of the host infants, and fibroblasts of the fetuses, as well as from lymphocytes of the parents. Six small pieces of fetiform tissues in FIF-2 were unavailable for the present study. A total of 38 microsatellite markers on the ABI Prism Linkage Mapping Set MD-10 (Panels 11, 12, 21, 22, 23, and 24; Applied Biosystems, Foster City, CA) were used to genotype Host 1, F-1a and F-1b, and 26 such markers (Panels 21 and 22) for Host 2 and F-2. DNA was amplified by PCR, and PCR products were analyzed on 3100 Genetic Analyzer™ (Applied Biosystems).

Microarray Analysis of Single Nucleotide Polymorphism (SNP) Loci

We used GeneChip Human Mapping 50K Array Xba™ (Affymetrix, Inc., Santa Clara, CA) for SNP genotyping. Genomic DNA (250 ng) was digested with *XbaI* (New England Biolabs, Beverly, MA), ligated by adaptor *XbaI* (Affymetrix), and subjected to PCR using primers (GeneChip Human Mapping 50K Xba Assay Kit™, Affymetrix) with conditions of 94°C for 3 min followed by initial denaturation of 94°C for 30 sec, 60°C for 45 sec, and 68°C for 60 sec

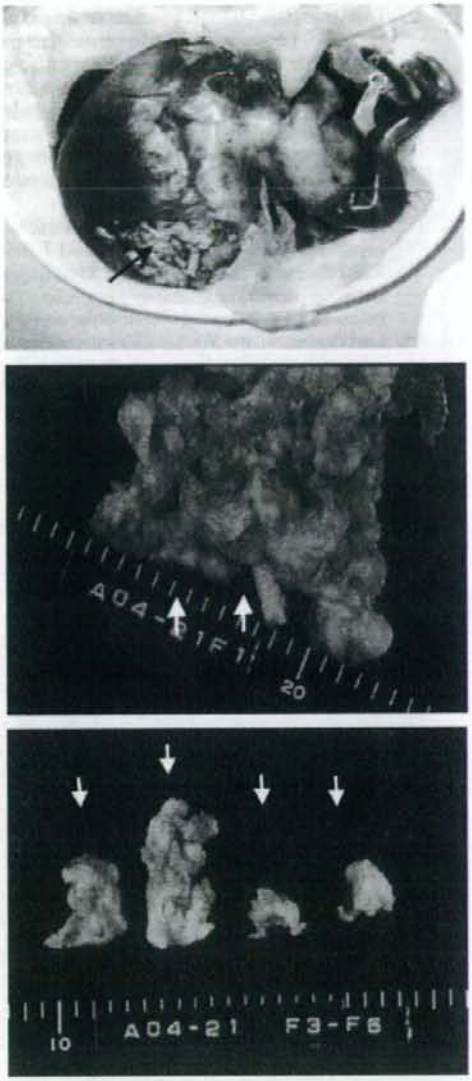

FIG. 2. FIF-2. **a**: A male infant having an intracranial fetus-like organ (arrow). **b** and **c**: Six irregular fetiform tissues (arrow) in addition to the intracranial fetus as shown in (**c**). [Color figure can be viewed in the online issue, which is available at www.interscience.wiley.com.]

for 30 cycles, and by final extension of 68°C for 7 min. PCR products were purified, fragmented using fragmentation reagents (Affymetrix), end-labeled with terminal deoxynucleotidyl transferase, and hybridized onto 50K Mapping Array™ (Affymetrix) at 48°C for 16 hr at 60 rpm. The hybridized array was washed and stained on Fluidics Station 450™ and scanned with GeneChip Scanner™

(Affymetrix). The arrays were analyzed with software GDAS™ version 3.0.2 (Affimetrix) that provides rank scores for the probability of particular genotypes at SNP loci. The scores for homozygous alleles are "AA" or "BB" call and for heterozygous alleles "AB" call, and confidence scores show the accuracy of the genotype call. We chose SNPs showing discordancy (each confidence score of <0.1) between the host infants and their fetuses.

Prior to the GeneChip analysis, we tested whether a given SNP call could be changed before and after *Xba*I digestion, because uncut *Xba*I fragments would show a seemingly aberrant allele. Two pairs of primers (a SNP and its upstream sites, and the SNP and downstream *Xba*I sites) were designed (Fig. 3a). After DNA from Host 1, F-1a and F-1b was digested with *Xba*I, it was amplified with PCR and sequenced under conditions above. Consequently, 12 *Xba*I sites randomly selected were confirmed in situ, and genotypes of Host 1 always corresponded those of F-1a and F-1b.

Regions of SNPs discordant between the host infants and their fetuses in the GeneChip analysis were sequenced in order to confirm the results. PCR was performed with primers generated for both sides of SNP sites using 2 μl of DNA, 10× PCR buffer, GeneAmp™ dNTP Mix (Applied Biosystems), and 0.5 μl of AmpliTaq Gold™ (Applied Biosystems). PCR conditions were 94°C for 10 min, and 30 cycles of 94°C for 30 sec, 60°C for 30 sec, and 72°C for 30 sec, followed by final extension at 72°C for 10 min. PCR products were analyzed by agarose gel electrophoresis and then sequenced on 3100 Genetic Analyzer (Applied Biosystems).

Methylation Assay at the *IGF2-H19* Locus

Methylation status of the differentially methylated region (*DMR*) at the human *IGF2-H19* locus at chromosome 11p15.5 was analyzed in the two cases of FIF. To differentiate parental alleles in the host infants and their fetuses, we adopted an 8097A/G SNP (Genbank Access No. AF125183, rs2107425) within *DMR* (Fig. 3b). Primer sequences (5′-3′) were as follows [Poon et al., 2002]: forward, GGACGGAATTGGTTGTAGTT; and reverse, AGG-

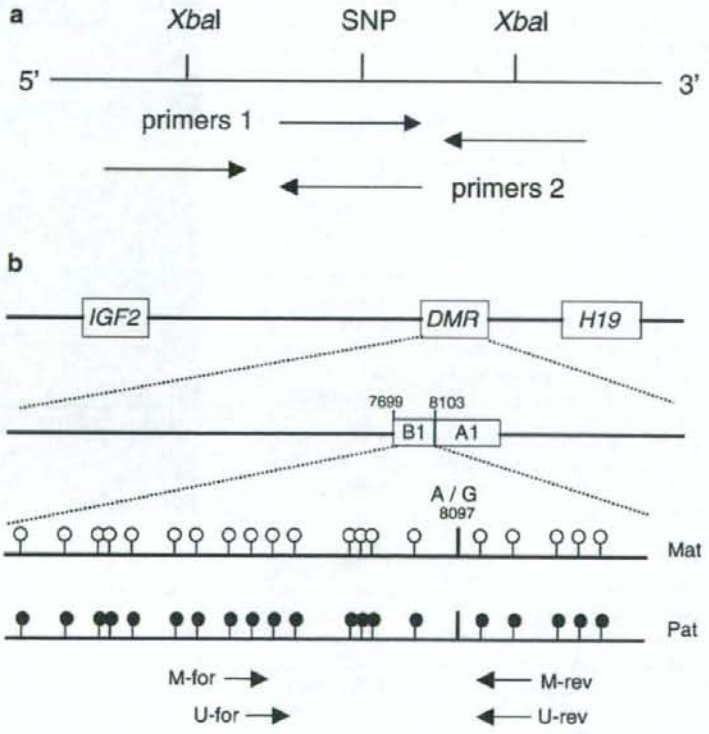

FIG. 3. **a**: *Xba*I sites around a putative SNP call for GeneChip Human Mapping 50K Array (Affymetrix) and primers designed to detect the SNP. Arrows indicate primer location and direction. **b**: Genomic structure and differentially methylated region (*DMR*) of the human *IGF2-H19* locus at 11p15.5. Numbers above bars show nucleotide numbers. Open and closed lollipops depict unmethylated and methylated regions in maternally (Mat) and paternally (Pat) derived normal chromosomes 11, respectively. Arrows indicate primer location and direction.

CAATTGTCAGTTCAGTAA. PCR was performed using Gene Amp™ PCR system 9700 (Applied Biosystems) with the conditions of 2 min at 95°C, and 35 cycles of 1 min at 95°C, 20 sec at 56°C, 20 sec at 72°C, and 10 min at 72°C. PCR products were analyzed by agarose gel electrophoresis, and sequenced by 3100 Genetic Analyzer™ (Applied Biosystems).

DNA was modified with sodium bisulfite [Kubota et al., 1997] using CpGenome™ DNA Modification Kit (Chemicon International, Temicula, CA) as instructed by the manufacturer. After conversion of DNA, the methylation status of *DMR* was examined. Methylation-specific PCR was performed in a 10 μl mixture containing 1 μl of modified DNA, 1 μl of 10× PCR buffer, 0.8 μl of GeneAmp™ dNTP Mix (Applied Biosystems), each of 1 μl forward and reverse primers, and 0.05 μl of AmpliTaq Gold™ (Applied Biosystems) under conditions of initial denaturation at 95°C for 12 min followed by 60 cycles of 95°C for 45 sec, 55°C (or 49°C) for 20 sec, and 72°C for 20 sec. Sequences (5′-3′) of primers designed by Poon et al. [2002] are as follows: M-for, TTAATTGGGGTTC-GTTCG: M-rev, CCCGACCTAAAAATCTAATACGA; U-for, GGTTTGTTTGTGGAAATGTTTT; and U-rev, CCCAACCTAAAAATCTAATACAA. PCR products were cloned using TOPO TA cloning Kit™ (Invitrogen, Carlsbad, CA) and sequenced on 3100 Genetic Analyzer.

RESULTS

Genotypes of Host Infants and Their Fetuses

Eleven of 38, and 13 of 26 microsatellite markers used for genotyping were informative in FIF-1 and FIF-2, respectively (Table I). Genotype analysis showed that at any informative locus, Host 1, F-1a and F-1b all inherited one copy of each parental allele, and their genotypes were all identical. The same results were obtained in Host 2 and F-2. As for the microarray analysis, the overall SNP call rate was more than 95%, indicating that all experimental steps had worked well. Host 1, and F-1a and F-1b seemed discordant (confidence < 0.1) for genotypes at 52 of some 50,000 SNP loci examined, although F-1a and F-1b were concordant at all these loci. However, sequence-based genotyping at 13 SNP loci that were randomly chosen from the 52 SNP regions showed complete concordance among the three subjects (Table II). There were no discordant alleles examined between Host 2 and F-2.

Methylation Status of *DMR* in Host Infants and Their Fetuses

Analysis of a *DMR*-SNP in FIF-1 showed that the mother was an AA homozygote, the father a GA heterozygote, and Host 1, F-1a and F-1b were all GA heterozygotes (Table III). Thus alleles A and G in the children were maternally and paternally derived, respectively. Likewise in FIF-2, the mother was a GG homozygote, the father an AA homozygote, and both Host 2 and F-2 GA heterozygotes, indicating that the children inherited one maternal and one paternal allele (Table III).

TABLE I. Genotypes at Microsatellite Marker Loci of Two Cases of FIF

FIF-1	Markers	Mother	Father	Host 1	F-1a	F-1b
	D16S3075	2,2	1,3	1,2	1,2	1,2
	D16S3136	1,2	3,4	2,3	2,3	2,3
	D16S520	2,3	1,2	1,3	1,3	1,3
	D15S131	2,4	1,3	2,3	2,3	2,3
	D16S503	2,2	1,3	1,2	1,2	1,2
	D16S423	1,2	3,4	1,3	1,3	1,3
	D15S1007	3,3	1,2	1,3	1,3	1,3
	D7S669	1,2	1,3	2,3	2,3	2,3
	D7S502	1,3	2,4	2,3	2,3	2,3
	D8S505	2,2	1,3	1,2	1,2	1,2
	D8S285	1,3	2,3	1,2	1,2	1,2
FIF-2	Markers	Mother	Father	Host 2	F-2	
	D16S3136	1,3	2,2	2,3	2,3	
	D15S130	2,2	1,1	1,2	1,2	
	D16S515	1,2	3,3	1,3	1,3	
	D15S1002	1,2	3,4	1,3	1,3	
	D16S503	3,4	1,2	2,3	2,3	
	D15S127	1,3	2,4	2,3	2,3	
	D15S153	1,4	2,3	3,4	3,4	
	D15S117	2,3	1,1	1,3	1,3	
	D16S3046	1,2	3,4	1,4	1,4	
	D15S205	2,3	1,3	1,2	1,2	
	D15S1012	3,3	1,2	1,3	1,3	
	D15S120	2,2	1,3	2,3	2,3	
	D15S128	1,3	2,4	1,2	1,2	

Analysis of the methylation status in *DMR* at the *IGF2-H19* locus was done by bisulfite treatment, and methylated or unmethylated sequence-specific PCR, followed by cloning of PCR products. Normally, only the paternal allele in *DMR* is methylated and the maternal allele remains unmethylated [Bartolomei and Tilghman, 1997]. This methylation pattern was altered in F-1a and F-1b. In F-1a, 8 (53.3%) of 15 clones showing unmethylated patterns had the maternally derived allele A and the remaining 7 (46.7%) had the paternally derived allele G (Table III). In F-1b, of nine such clones, three (33.3%) had the maternal and six (66.7%) had the paternal allele. On the contrary, the methylation status of Host 2 and F-2 were the same in all clones examined, showing normal patterns.

DISCUSSION

Prenatal US and MRI suggested that all three fetiform masses examined in our two cases contained vertebral columns, limb bones, and various soft tissues. The findings were confirmed by pathological analysis after birth, and ruled out teratomatous neoplasia but were consistent with FIF [Hoeffel

TABLE II. Thirteen SNP Markers, Genotypes Seemingly Discordant Between Host 1 and Two Fetuses (F-1a and 1b) by GeneChip Analysis, and Subsequent Confirmation of Concordancy by Sequencing Analysis

dbSNP ID	Chromosome	Primer	Sequence (5′-3′)	Genotype		
				Host 1	F-1a	F-1b
rs4131373	1	Forward	GCACAGTGGAGCTGCTGTTG	GG	GG	GG
		Reverse	GAGTTTGCTGAAGGCAGTGC			
rs960813	2	Forward	CGTGTTACCTTACTGTCCCT	GC	GC	GC
		Reverse	GTTCTGGTGTGTACTTTGCC			
rs4955768	3	Forward	CGATGAGGCATCTCATTACG	AA	AA	AA
		Reverse	TCTCTCTGTCCATCTGAAGG			
rs1951233	4	Forward	GCAATGATCACAGTGACTGAGG	AA	AA	AA
		Reverse	TGTGCTATTGTGGGTCTGCC			
rs60701	5	Forward	GAATCCCTTGGGTAGAACAC	TT	TT	TT
		Reverse	GGTGAATGCAGTAGTAGCCA			
rs2223995	6	Forward	CCAGCTCCACAATGAACCCA	TT	TT	TT
		Reverse	CCGTGCTTCCTAATGGTAGC			
rs1987475	7	Forward	GGAGCTCTGTGAGGAGCTGT	TT	TT	TT
		Reverse	CAAGCCCAGCTGAGCACCTT			
rs10503645	8	Forward	GCAAGAGTGTGGCTAGATCAC	CC	CC	CC
		Reverse	CCTGTTCCAGGCTGCCAGAT			
rs2077852	9	Forward	GACCTTCACCAGGACAACGT	GT	GT	GT
		Reverse	TTAGACCTTGTCAGGACGGC			
rs1159006	10	Forward	CATACCACAAGTCGTCGAGC	CT	CT	CT
		Reverse	CCTGCCAATCTAGAGGTAGG			
rs1036809	15	Forward	GGTCATCCTAGAGCAAGTCA	GC	GC	GC
		Reverse	GCACATCGTAGGGACTTAAG			
rs8587	16	Forward	CACGACCGACTGAACATTCT	AA	AA	AA
		Reverse	AAGCTGTCCTACACTTGTGC			
rs2067084	20	Forward	GCATGGTTCCTGGCATGCTG	CC	CC	CC
		Reverse	TCCACCAACCACTCTCTGTC			

et al., 2000; Brand et al., 2004]. Six separate fetiform tissues were observed in FIF-2, although we did not examine whether they had vertebral columns. Thus, in both of our cases of FIF, multiple fetuses-in-fetu were evident, as reported previously [Iyer et al., 2003]. Parthenogenetic origin or ovarian teratoma [Miura et al., 1999] was also totally ruled out in the two cases, because host infants were both males.

We have shown that in both cases analyzed host infants and their fetuses shared the same genotypes at all polymorphic loci examined. In other words, they originated from the same zygote. Our data support the monozygotic twin theory [Gilbert-Barness et al., 2003; Beaudoin et al., 2004; Brand et al., 2004]. However, a simple monozygotic (monochorionic, diamniotic) twin theory may not explain all cases of FIF. There have been some reports on the simultaneous presence of a fetus and teratoma [Magnus et al., 1999; Gilbert-Barness et al., 2003], multiple fetuses were involved in FIF [Iyer et al., 2003] as in our cases, fetiform mass was composed of underdeveloped organs or tissues [de Lagausie et al., 1997; Hopkins et al., 1997], and such mass grew in any body part of a fetus [Afshar et al., 1982; Magnus et al., 1999; Beaudoin et al., 2004; Borges et al., 2005]. A monozygotic, dichorionic, diamniotic twin theory [Beaudoin et al., 2004] may answer the questions. Normally, 30 hr after fertilization, a zygote consists of two cells, but if a zygote divides into two separate embryos, they may become monozygotic, dichorionic, diamniotic twins. Subsequently, around the 5th day of development, if one blastocyst that is derived from one conceptus is implanted into the other blastocyst instead of normal implantation into the uterine endometrium, or the former blastocyst is enclosed by the latter if they are implanted closely, and such an implant or inclusion body may not develop normally, leading to FIF. From an embryological point of view, the existence of the vertebral column in fetiform mass may reflect its derivation from a primitive streak. The formation of the primitive streak normally starts during the 3rd week, together with gastrulation that will lead to the notochord formation and subsequently to the

TABLE III. Genotypes of a SNP in the DMR at the *IGF2-H19* Locus and Methylated or Unmethylated Alleles After Bisulfite Conversion

Cases	Family members	Genotypes	Alleles	
			Methylated	Unmethylated (% of clones)
FIF-1	Mother	AA	A	A
	Father	GA	A	G (100)
	Host 1	GA	G	A (100)
	F-1a	GA	G	A (53.3), G (46.7)
	F-1b	GA	G	A (33.3), G (66.7)
FIF-2	Mother	GG	G	G
	Father	AA	A	A
	Host 2	GA	A	G (100)
	F-2	GA	A	G (100)

vertebral column and segmental axis. Thus, FIF likely arises from a zygote at a primitive-streak stage and fetiform mass develops to a certain degree in a manner similar to normal fetal development.

In our FIF-1, methylated patterns of F-1a and F-1b at the *IGF2-H19* locus were different from their host infant. Although the detailed methylation status at this locus during early human development has remained obscure, parental imprints in mice are erased once during gametogenesis [Reik et al., 2001; Li, 2002] and an early embryo is unmethylated and gradually begins to be methylated during blastocyst stage [Reik et al., 2001; Li, 2002]. In FIF-1, two isolated blastocysts originating from one zygote may have been implanted into (or included by) the other host blastocyst during a process of establishing methylation. The reprogramming of methylation in the two abnormally implanted embryos may have not proceeded thereafter by certain unknown mechanisms such as tumorization. Ovarian tumors from various stages of oogenesis do maintain their methylation status at their original stage [Miura et al., 1999]. On the other hand, such abnormal implantation may have occurred in FIF-2 after the establishment of methylation, since methylation patterns in Host 2 and F-2 were identical.

Thus, we may have provided another line of evidence that the FIF anomaly is of monozygotic origin. This is the first case of FIF showing different methylation patterns between a host infant and fetiform mass. Our data of the methylation analysis will contribute to future studies on pathogenesis of FIF.

ACKNOWLEDGMENTS

This study was supported by Grants-in-Aid for Scientific Research (Category C, 16591670 for K. M. and Category C, No. 17591748 for H. M.), Grant-in-Aid on Priority Areas "Applied Genomics" (No. 17019055 for N. N.) from the Ministry of Education, Sports, Culture, Science and Technology of Japan, and by SORST from Japan Science and Technology Agency (JST) (for N. N.)

REFERENCES

Afshar F, King TT, Berry CL. 1982. Intraventricular fetus-in-fetu. J Neurosurg 56:845–849.

Bartolomei MS, Tilghman SM. 1997. Genomic imprinting in mammals. Annu Rev Genet 31:493–525.

Beaudoin S, Gouizi G, Mezzine S, Wann AR, Barbet P. 2004. Mediastinal Fetus in fetu case report and embryological discussion. Fetal Diagn Ther 19:453–455.

Borges E, Lim-Dunham JE, Vade A. 2005. Fetus in fetu appearing as a prenatal neck mass. J Ultrasound Med 24:1313–1316.

Brand A, Alves MC, Saraiva C, Loio P, Goulao J, Malta J, Palminha LM, Martins M. 2004. Fetus in fetu-Diagnostic criteria and differential diagnosis—A case report and literature review. J Pediatr Surg 39:616–618.

Chen CP, Chern SR, Liu FF, Jan SW, Lee HC, Sheu JC, Lee WT, Wang TY. 1997. Prenatal diagnosis, pathology, and genetic study of fetus in fetu. Prenat Diagn 17:13–21.

de Lagausie P, de Napoli Cocci S, Stempfle N, Truong QD, Vuillard E, Ferkadji L, Aigrain Y. 1997. Highly differentiated teratoma and fetus-in-fetu: A single pathology? J Pediatr Surg 32:115–116.

Eng HL, Chuang JH, Lee TY, Chen WY. 1989. Fetus in fetu: A case report and review of the literature. J Periatr Surg 24:296–299.

Gilbert-Barness E, Opitz JM, Debich-Spicer D, Muller T, Arnold SR, Quintero R. 2003. Fetus-in-fetu form of monozygotic twinning with retroperitoneal teratoma. Am J Med Genet Part A 120A:406–412.

Heifetz SA, Alrabeeah A, Brown BS, Lau H. 1988. Fetus in fetu: A fetiform teratoma. Pediatr Pathol 8:215–226.

Higgins KR, Coley BD. 2006. Fetus in fetu and fetiform teratoma in 2 neonates: An embryologic spectrum? J Ultrasound Med 25: 259–263.

Hing A, Corteville J, Foglia RP, Bliss DP Jr, Donis-Keller H, Dowton SB. 1993. Fetus in fetu: Molecular analysis of a fetiform mass. Am J Med Genet 47:333–341.

Hoeffel CC, Khoag QN, Tran TT, Fornes P. 2000. Fetus in fetu: A case report and literature review. Pediatrics 105:1335–1344.

Hopkins KL, Dickson PK, Ball TI, Ricketts RR, O'Shea PA, Abramowsky CR. 1997. Fetus-in-fetu with malignant recurrence. J Pediatr Surg 32:1476–1479.

Iyer KV, Vinaya K, Haller JO, Maximin S, Barrerras J, Velchek F. 2003. Multiple fetuses in fetu: Imaging findings. Pediatr Radiol 33:53–55.

Kubota T, Das S, Christian SL, Baylin SB, Herman JG, Ledbetter DH. 1997. Methylation-specific PCR simplifies imprinting analysis. Nat Genet 16:16–17.

Kumar AN, Chandak GR, Rajasekhar A, Reddy NCK, Singh L. 1999. Fetus-in-fetu: A case report with molecular analysis. J Pediatr Surg 34:641–644.

Li E. 2002. Chromatin modification and epigenetic reprogramming in mammalian development. Nat Rev Genet 3:662–673.

Lord JM. 1956. Intra-abdominal foetus in foetu. J Pathol Bacteriol 72:627–641.

Magnus KG, Millar AJ, Sinclair-Smith CC, Rode H. 1999. Intrahepatic fetus-in-fetu: A case report and review of the literature. J Pediatr Surg 34:1861–1864.

Miura K, Obama M, Yun K, Masuzaki H, Ikeda Y, Yoshimura S, Akashi T, Niikawa N, Ishimaru T, Jinnno Y. 1999. Methylation imprinting of H19 and SNRPN gene in human benign ovarian teratomas. Am J Hum Genet 65:1359–1367.

Naudin ten Cate L, Vermeij-Keers C, Smit DA, Cohen-Overbeek TE, Gerssen-Schoorl KBJ, Dijkhuizen T. 1995. Intracranial teratoma with multiple fetuses: Pre- and post-natal appearance. Hum Pathol 26:804–807.

Ouimet A, Russo P. 1989. Fetus in fetu or not? J Pediatr Surg 24:926–927.

Poon LLM, Leung TN, Lau TK, Chow KCK, Lo YMD. 2002. Differential DNA methylation between fetus and mother as a strategy for detection fetal DNA in maternal plasma. Clin Chem 48:135–141.

Reik W, Dean W, Walter J. 2001. Epigenetic reprogramming in mammalian development. Science 293:1089–1093.

Willis RA. 1935. The structure of teratoma. J Pathol Bacteriol 40: 1–36.

Congenital Neuroblastoma in a Patient With Partial Trisomy of 2p

Yuri Dowa, MD, Toshiyuki Yamamoto, MD,* Yasuko Abe, MD,† Masaki Kobayashi, MD,‡ Rikuo Hoshino, MD,‡ Kazumi Tanaka, MD,§ Noriko Aida, MD,‖ Hiroshi Take, MD,¶ Keisuke Kato, MD,# Yukichi Tanaka, MD,# Jyunpei Ariyama,** Naoki Harada,** Naomichi Matsumoto, MD,†† and Kenji Kurosawa, MD**

Summary: We report the fourth example of a patient with germline partial trisomy of 2p21-pter and congenital neuroblastoma. The male infant had a dysmorphic facial expression and presented with congenital heart disease, supernumerary nipples, hypospadias, shawl scrotum, hemilateral persistent hyperplastic primary vitreous, and neuroblastoma. His germline karyotype of 46,XY,der(8)t(2;8)(p21;p23.2) was inherited from a maternal-balanced translocation, which indicates that the proto-oncogene *MYCN* region of 2p24.3 is tripicated in germline cells. A cytogenetic study of the biopsied tumor cells did not show *MYCN* amplification, but the DNA index was 2.4 and histologic fluorescent in situ hybridization analysis indicated somatic mutation with near-pentaploidy of the tumor cells. This could be an alternative mechanism of *MYCN* activation in the process of the tumorigenesis of neuroblastoma.

Key Words: neuroblastoma, *MYCN*, 2p trisomy, translocation

(*J Pediatr Hematol Oncol* 2006;28:379–382)

In Japan, neuroblastoma is the most common malignant solid tumor in childhood and accounts for 10% of all cases of childhood cancer.[1] Eighty percent of cases are diagnosed before the age of 5 years, with a mean age at diagnosis of 2 years. The tumor arises from primitive neural crest cells that form the adrenal medulla and sympathetic nervous system. Cytogenetic and molecular analysis of neuroblastoma has identified several structural chromosomal aberrations, including amplification of *MYCN* (a member of the MYC gene family), loss of 1p36, and gain of 17q.[1] It is now estimated that approximately 25% of neuroblastomas carry amplified *MYCN*, making this gene one of the most reliable prognostic factors for neuroblastoma. Normally, only a single copy of *MYCN* resides on chromosome 2.

Partial trisomy of 2p was first reported over 30 years ago.[2] Lurie et al[3] recently reviewed over 50 cases, including 3 new reports. Characteristic clinical features include anomalies of the face, trunk, limbs, and genitalia, and psychomotor delay. Other congenital defects that seem to be associated with this trisomy involve the neural tube, lung, heart, and diaphragm. Thus far, there have been 3 reports of partial trisomy of 2p associated with congenital neuroblastoma.[4–6] Recently, we encountered an additional patient having the partial 2p trisomy syndrome associated with neuroblastoma.

PATIENT REPORT

The patient was the second child of nonconsanguineous parents. The first son was healthy and the mother had a history of ovarian cancer. Prenatal examination by ultrasonography revealed a fetal double-outlet right ventricle (DORV) and a ventricle septum defect (VSD). Intrauterus growth retardation was detected in the third trimester. The male child was delivered by forceps at 37-week gestation after induction for nonreassuring fetal heart rate. At birth, the child showed severe intrauterus growth retardation, with a weight of 1776 g (−1.7 SD), height of 41 cm (−3.4 SD), and head circumference of 31 cm (−1.0 SD). He was intubated immediately because of respiratory distress that developed after birth. Significant physical findings consisted of unusual facial features with a prominent forehead, hypertelorism, a depressed nasal bridge, and posteriorly angulated ears (Fig. 1A). Supernumerary nipples, hypospadias, and a shawl scrotum were also noted (Fig. 1B). The prenatally detected congenital heart defect with DORV and VSD was confirmed by ultrasonographic examination, as was pulmonary stenosis.

The child was extubated at postnatal day 7. From 13 days of age, his abdomen began slowly distending, and the liver was palpable 2 cm under the costal arch. When the patient was 1 month old, abdominal ultrasonography and an abdominal computed tomography (CT) scan revealed a retroperitoneal mass and intrahepatic tumor (Fig. 1C). A biopsy was obtained from the metastatic tumor in the liver, and the findings of the pathologic examination were consistent with stage 4S neuroblastoma, poorly differentiated type, and favorable histology, according to the Shimada System (Figs. 1D, E).[1]

At 8 months, the patient had opacification of the left lens and aspiration was performed via the corneal limbus. We also

Received for publication September 6, 2005; accepted April 7, 2006.
From the Departments of *Medical Genetics, †Oncology, ‡Neonatology, §Ophthalmology, ‖Radiology, ¶Surgery, and #Pathology, Kanagawa Children's Medical Center; ††Department of Human Genetics, Yokohama City University Graduate School of Medicine, Yokohama; and **Kyushu Medical Science Nagasaki Laboratory Inc, Nagasaki, Japan.

Reprints: Toshiyuki Yamamoto, MD, International Research and Educational Institute for Integrated Medical Sciences (IREIIMS), Tokyo Women's Medical University, 8-1 Kawada-cho, Shinjuku-ku, Tokyo, 162-8666, Japan (e-mail: yamamoto@imcir.twmu.ac.jp).

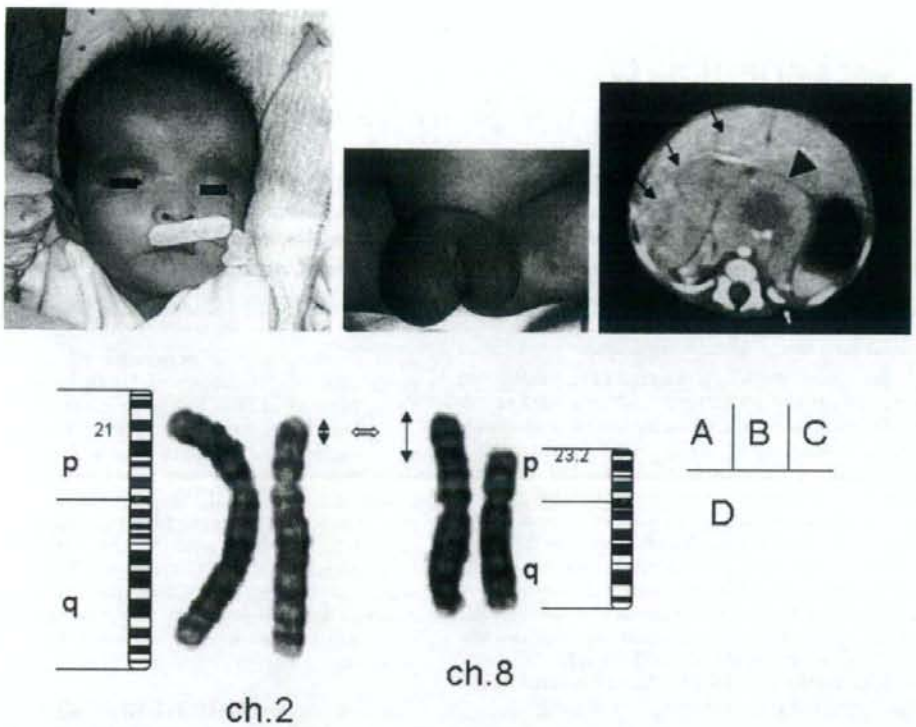

FIGURE 1. Photographs of dysmorphic facial appearance (A) and shawl scrotum (B) at 2 months of age. A large retroperitoneal mass (arrowhead) surrounding the abdominal aorta with punctual calcifications is shown by contrast-enhanced computed tomography (C). The enlarged right lobe of the liver including metastatic masses with irregular margin (arrows) can be seen. G-banded partial karyotype of chromosomes 2 and 8 of the mother (D). Derivative chromosomes are inside, which indicate the karyotype of the patient as 46,XY,der(8)t(2;8)(p21;p23.2)mat.

detected abnormal vascularization from the posterior element of the left lens, indicating that the secondary cataract was induced by persistent hyperplastic primary vitreous (PHPV).[7]

He has been receiving primary chemotherapy with low-dose cyclophosphamide and vincristine, and now he is 1.5 years old without any progression of the neuroblastoma.[8] However, he showed severe psychomotor developmental delay as he had never sat up alone, and had been fed by tube because of feeding difficulty.

CYTOGENETIC STUDIES

The clinical features were suggestive of a partial 2p trisomy, and a cytogenetic study was performed using his peripheral leukocytes. Routine G-banded chromosome analysis showed a male karyotype with a derivative chromosome 8 with unknown origin on the short arm. To confirm the origin of this additional region, parental karyotypes were analyzed. His father's karyotype was normal with 46,XY, and his mother showed reciprocal translocation between 2p and 8p with a karyotyping 46,XX,t(2;8)(p21;p23.2) (Fig. 2A). Detailed fluorescent in situ hybridization (FISH) analyses using BAC/PAC clones were performed to detect the breakpoint of each chromosome, according to a method described elsewhere.[9] BAC/PAC clones of RP11-24K2, RP11-128C5, RP11-72C11, RP11-633O21, RP11-819H19, RP11-907L18, RP11-130P22, and RP11-91C18 on the short arm of chromosome 2, and RP11-412I11, RP11-121F7, RP11-590N22, RP11-243D4, RP11-89I12, RP11-296E5, RP11-3N20, RP11-143D15, and RP11-118D21 on the short arm of chromosome 8 were selected by the UCSC genome browser (http://genome.ucsc.edu/). The patient's final karyotype was determined to be 46,XY,der(8)t(2;8)(p21;p23.2)mat. ish der(8)t(2;8)(p21;p23.2)(RP11-24K2+,RP11-128C5+,RP11-72C11+,RP11-633O21+,RP11-819H19+,RP11-907L18+,RP11-130P22−,RP11-91C18−,RP11-412I11−,RP11-121F7−,RP11-590N22+,RP11-243D4+,RP11-89I12+,RP11-296E5+,RP11-3N20+,RP11-143D15+,RP11-118D21+). This result indicates partial trisomy of 2p21-pter, in which *MYCN* is included, and partial monosomy of 8p23.2-pter, not including the locus of *GATA4*.

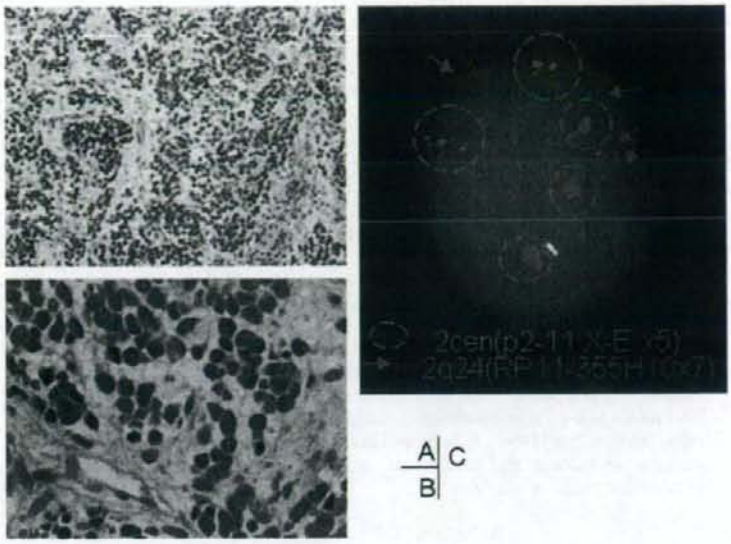

FIGURE 2. Pathologic examination with hematoxylin/eosin staining, ×10 (A) and ×40 (B). The wedge-resected tissue showed nests of neuroblastic cells with neurofibrillary matrix delineated by edematous stroma with hepatic cell cords. The stroma was composed of a fine eosinophilic matrix, but the Schwannian stroma was less developed. Mitoses and karyorrhexis were observed at a rate less than 2% of the entire neoplastic cells. Histologic FISH analysis of touch imprint of the biopsy specimens (C). Signals from probes for the chromosome 2 centromere (D2Z1) and *MYCN* are visible, with 5 and 7 signals, respectively, per cell.

Slot-blot hybridization analysis of biopsy specimens to detect gene amplification of *MYCN* did not show amplification (SRL, Tokyo). However, a *MYCN* proto-oncogene DNA index of 2.4 was obtained (SRL, Tokyo). Further histologic FISH analysis of a touch imprint of the tumor was performed using a chromosome 2 centromere probe prepared from p2-11 *X-E* (a generous gift from Dr H.F. Willard) and a *MYCN* probe prepared from RP11-355H10 (BAC/PAC Resources Center, Children's Hospital Oakland Research Institute, CA). The result showed that most of the neoplastic cells displayed 3 to 7 signals of the chromosome 2 centromere and 5 to 9 signals of *MYCN*. The median observations were 5 signals of the chromosome 2 centromere and 7 signals of *MYCN*, indicating somatic mutation with near-pentaploidy of the tumor cells (Fig. 2B).

DISCUSSION

The patient's characteristic clinical features of a prominent forehead, hypertelorism, a depressed nasal bridge, posteriorly angulated ears, hypospadias, and a shawl scrotum are compatible with partial duplication of chromosome 2p. This patient developed neuroblastoma within a month after birth and a secondary cataract induced by PHPV at the age of 8 months. This is the fourth report of partial 2p trisomy syndrome associated with neuroblastoma. Previous studies have found that associated chromosomal deletions in these patients were variable and included 13q34, 16p11, and 8p23.[4–6] However, triplication of *MYCN* in the germline cells (in the triplicated region of 2p24.3) was common to all 4 patients (Table 1).

In 1983, Schwab et al[10] reported the amplification of *MYCN* in neuroblastoma cell lines and in 1 tumor. In 1984, Brodeur and colleagues[11] reported the correlation of *MYCN* amplification with advanced-stage disease. Clinical studies have confirmed that amplification of the *MYCN* proto-oncogene is one of the best prognostic indicators of poor outcome.[12] Although approximately 30% of neuroblastoma tumors present *MYCN* amplification at diagnosis, FISH studies have recently shown that *MYCN* is occasionally duplicated at its resident site in neuroblastoma cell lines without further amplification, suggesting that it could be an alternative mechanism of *MYCN* activation.[13,14] However, only 4 patients with trisomy 2p showing congenital neuroblastoma have thus far been reported.[4–6]

The present patient also had a partial monosomy of 8p23.2-pter. There are many reported patients with small

TABLE 1. Summary of Germline 2p Trisomy Associated With Neuroblastoma

	Duplicated Region	Deleted Region	Origin	Neuroblastoma	The Other Combined Symptoms
Patel et al[6]	2p23-pter	13q34-qter	Unknown	+	Postaxial polydactyly, seizures
Our patient	2p21-pter	8p23.2-pter	Maternal	+	DORV, VSD, PS, hypospadias, shawl scrotum, cataract, severe mental retardation
Say et al[4]	2p21-p25	—	Unknown	+	Lung agenesis, dead at 35 d
Nagano et al[5]	2p13-pter	16p11-pter	Paternal	+	Microphthalmos, congenital cataract, micropenis

distal 8p deletions.[15,16] The findings in these patients suggest that major congenital anomalies, especially congenital heart defects, are frequent, but facial dysmorphism may be subtle and mental retardation less severe than in those with deletions associated with more proximal breakpoints.[15,16] Mutations and haploinsufficiency of *GATA4* in this region with 8p23.1 have been shown to be responsible for congenital heart defects.[17,18] According to our detailed FISH study, the locus of *GATA4* is at least 8 Mb proximal from the breakpoint of 8p23.2. Thus, congenital heart defects associated with DORV, VSD, and pulmonary stenosis of this patient, cannot be explained by haploinsufficiency of *GATA4*.

In patients with PHPV, the primary vitreous and embryonic vitreous vasculature remains and grows even after birth, although it is generally isolated and unilateral. The incidence of this condition is unknown, but it is not rare. Although PHPV has been associated with numerous genetic syndromes, the mechanism contributing to these conditions remains unclear.[19]

REFERENCES

1. Brodeur G, Sawada T, Tsuchida Y, et al. *Neuroblastoma*. Amsterdam: Elsevier; 2000.
2. Bender K, FAU-Reinwein H, Gorman LZ, et al. Familial 2-C translocation: 46,XYt(2p-;Cp+) and 46,XXCp+. *Humangenetik*. 1969;8:94–104.
3. Lurie IW, Ilyina HG, Gurevich DB, et al. Trisomy 2p: analysis of unusual phenotypic findings. *Am J Med Genet*. 1995;55:229–236.
4. Say B, Carpenter NJ, Giacoia G, et al. Agenesis of the lung associated with a chromosome abnormality (46,XX,2p+). *J Med Genet*. 1980;17:477–478.
5. Nagano H, Kano Y, Kobuchi S, et al. A case of partial 2p trisomy with neuroblastoma. *Jinrui Idengaku Zasshi*. 1980;25:39–45.
6. Patel JS, Pearson J, Willatt L, et al. Germline duplication of chromosome 2p and neuroblastoma. *J Med Genet*. 1997;34:949–951.
7. Dass AB, Trese MT. Surgical results of persistent hyperplastic primary vitreous. *Ophthalmology*. 1999;106:280–284.
8. Rubie H, Coze C, Plantaz D, et al. Localised and unresectable neuroblastoma in infants: excellent outcome with low-dose primary chemotherapy. *Br J Cancer*. 2003;89:1605–1609.
9. Shimokawa O, Kurosawa K, Ida T, et al. Molecular characterization of inv dup del(8p): analysis of five cases. *Am J Med Genet A*. 2004;128:133–137.
10. Schwab M, Alitalo K, Klempnauer KH, et al. Amplified DNA with limited homology to myc cellular oncogene is shared by human neuroblastoma cell lines and a neuroblastoma tumour. *Nature*. 1983;305:245–248.
11. Brodeur GM, Seeger RC, Schwab M, et al. Amplification of N-myc in untreated human neuroblastomas correlates with advanced disease stage. *Science*. 1984;224:1121–1124.
12. Bown N. Neuroblastoma tumour genetics: clinical and biological aspects. *J Clin Pathol*. 2001;54:897–910.
13. Corvi R, Savelyeva L, Schwab M. Duplication of N-MYC at its resident site 2p24 may be a mechanism of activation alternative to amplification in human neuroblastoma cells. *Cancer Res*. 1995; 55:3471–3474.
14. Valent A, Le Roux G, Barrois M, et al. MYCN gene overrepresentation detected in primary neuroblastoma tumour cells without amplification. *J Pathol*. 2002;198:495–501.
15. Hutchinson R, Wilson M, Voullaire L. Distal 8p deletion (8p23.1—8pter): a common deletion? *J Med Genet*. 1992;29:407–411.
16. Wu BL, Schneider GH, Sabatino DE, et al. Distal 8p deletion (8)(p23.1): an easily missed chromosomal abnormality that may be associated with congenital heart defect and mental retardation. *Am J Med Genet*. 1996;62:77–83.
17. Garg V, Kathiriya IS, Barnes R, et al. GATA4 mutations cause human congenital heart defects and reveal an interaction with TBX5. *Nature*. 2003;424:443–447.
18. Hirayama-Yamada K, Kamisago M, Akimoto K, et al. Phenotypes with GATA4 or NKX2.5 mutations in familial atrial septal defect. *Am J Med Genet A*. 2005;135:47–52.
19. Pellegrino JE, Engel JM, Chavez D, et al. Oculo-palatal-cerebral syndrome: a second case. *Am J Med Genet*. 2001;99:200–203.

Neuroradiologic Findings in Sotos Syndrome

ABSTRACT

Sotos syndrome is a well-known anomaly syndrome characterized by overgrowth, characteristic facial gestalt, and developmental delay, and haploinsufficiency of the *NSD1* gene has been revealed as one of the major genetic causes. However, there have been only a few reports on neuroradiologic findings by computed tomography (CT) or magnetic resonance imaging (MRI), and functional examination of the brain has not been reported. We examined three cases with typical Sotos syndrome, which also were confirmed by genetic analysis with a specific probe for the *NSD1* gene. The results of MRI showed the characteristic features that have been reported previously. The findings obtained by using single-photon emission computed tomography and magnetic resonance spectroscopy suggested an association between mental delay and behavioral tendency in Sotos syndrome and immaturity in frontal brain function. (*J Child Neurol* 2006;21:614–618; DOI 10.2310/7010.2006.00145).

Sotos syndrome is an anomaly syndrome characterized by overgrowth, characteristic facial gestalt, and developmental delay.[1,2] Recently, haploinsufficiency of the *NSD1* gene was revealed as one of the major genetic causes of Sotos syndrome.[3] From the first report by Sotos et al, more than 200 cases have been reported to date, but there have been only a few reports on neuroradiologic findings by computed tomography (CT) or magnetic resonance imaging (MRI).[1,4,5] Moreover, functional examination by using single-photon emission computed tomography (SPECT) or magnetic resonance spectroscopy has not been reported. We report here the neuroradiologic findings of three patients with Sotos syndrome examined by MRI, SPECT, and magnetic resonance spectroscopy, suggesting an immaturity in frontal brain function.

Case Reports

Case 1

A 3.5-year-old boy was referred for evaluation of his large body size and slow mental and motor development. His height and weight were around the +5 SD line but parallel with the average growth line. The pregnancy was uneventful, and he was born at 38 weeks with mild asphyxia and had moderate jaundice requiring phototherapy. His weight at birth was 4006 g (+2.0 SD), but data regarding his height and head circumference at birth were not obtained. He showed poor sucking ability owing to a cleft palate and remained in hospital until 45 days of age. Further, he could not hold his head up until 10 months. There was no family history of mental deficiency or gigantism. On examination, his height was 119 cm (+5.4 SD), equal to that of an average 7-year-old boy. He had a dolichocephalic head, which measured 57.5 cm (+5.0 SD), and there was frontal bossing and a prominent jaw. The cleft palate had been operated on. His eyes were widely spaced, and his hands and feet were large. His bone age was as advanced as that of a 7-year-old child. Eye funduscopic examination revealed no abnormal findings. He could sit but could not stand without help. He was unable to speak any significant words, and his developmental quotient, evaluated by the Enjouji Developmental Scale for Japanese children, was 34. He demonstrated significant instability of temper and was aggressive toward other people. The aggressiveness was triggered when he was contradicted. He frequently hit his own head on the floor.

Case 2

A 2-year-old boy was referred for evaluation of his slow mental and motor development. His height and weight were around the +2 SD line but parallel with the average growth line. The pregnancy had been uneventful, but he was born at 41 weeks by ceasarean section owing to his fetal asphyxia. His weight, height, and head circumference at birth were 4080 g (+2.2 SD), 53.5 cm (+1.5 SD), and 36.0 cm (+1.6 SD), respectively. He had mild jaundice that did not require phototherapy. He was unable to hold his head up until 5 months, and at 11 months, he still could not sit alone. At 18 months of age, he became able to walk unaided. There was no family history of mental deficiency or gigantism. On examination, his height was 90.8 cm (+2.0 SD), equal to that of an average

2.5-year-old boy. He had a dolichocephalic head, which measured 50.0 cm (+1.0 SD), frontal bossing, and a prominent jaw. His eyes were widely spaced, and his hands and feet were large, with fallen arches. His bone age was as advanced as that of a 3-year-old child. Eye funduscopic examination revealed no abnormal findings. He could walk alone but easily fell down. He was unable to speak any significant words, and his developmental quotient, evaluated by the Enjouji Developmental Scale for Japanese children, was 66. He demonstrated significant instability of temper and was aggressive toward other people, especially toward his mother. The aggressiveness was triggered when he was contradicted. He frequently hit his own head on a wall or pole. He developed myoclonic seizures at 4 years of age, and his electroencephalogram showed frequent spikes or spike-waves in the frontal region. The myoclonic seizures have been well controlled with clonazepam.

Case 3

A 2-year-old boy was referred for evaluation of his large body size and slow mental and motor development. His growth was slightly under the +2 SD line but parallel with the average growth line. The pregnancy and delivery were uneventful, but he was moderately jaundiced, and phototherapy was undertaken. His weight, height, and head circumference at birth were 3240 g (+0.1 SD), 51.0 cm (+1.4 SD), and 34.0 cm (+0.4 SD), respectively. He could hold his head up at 6 months, but his motor retardation and particular appearance were pointed out at this time. He was attending a local rehabilitation center for motor training. There was no family history of mental deficiency or gigantism. On examination, his height was 95 cm (+3.3 SD), equal to that of an average 3 ½-year-old boy. He had a dolichocephalic head, which measured 52 cm (+2.0 SD), and there was frontal bossing and a prominent jaw. The eyes were widely spaced, and the hands and feet were large, with fallen arches. Eye funduscopic examination revealed mild atrophic change of the optic nerves, which has been reported in Sotos syndrome.[6] His bone age was as advanced as that of a 4-year-old child. He could walk only if assisted. He could not speak any significant words, and his developmental quotient, evaluated by the Enjouji Developmental Scale for Japanese children, was 48. He did not demonstrate significant instability of temper or aggressiveness toward other people, but he sometimes hit his own head on a wall when he was contradicted.

Diagnosis

The characteristic facial gestalt, growth pattern, developmental delay, and accelerated bone age are the major diagnostic criteria for Sotos syndrome.[1,2] Chromosomal analysis with the conventional G-banding technique showed the normal karyotype, chromosome 46,XY, without any abnormalities, such as translocations. Recently, we revealed that haploinsufficiency of the *NSD1* gene is one of the major genetic causes of Sotos syndrome.[3] We also examined fluorescent in situ hybridization for the *NSD1* gene in the three patients here, and all of the results showed an absence of a fluorescent in situ hybridization signal for the PR1-118m12 probe containing the *NSD1* gene, along with the presence of five pter signals.[3]

Neuroradiologic Findings

Approval by research board of Gifu University Hospital and the informed consent of the patients' parents for the radiologic studies with sedation were obtained. MRI in the three cases showed ventricular abnormalities such as large global lateral ventricles, abnormal prominence of the trigone, and an occipital horn (Figure 1). In addition to these abnormalities, increased extracerebral fluid, midline structure abnormalities, thinning of the corpus callosum, cavum septum pellucidum, and cavum vergae were observed. These findings are similar to those in the previous report by Shaefer et al (Table 1).[4] There was no abnormal finding related to the optic nerve atrophy of case 3. Analysis of the brain SPECT using technetium-99m ethyl cysteinate dimer showed perfusion abnormalities in the two patients compared with the those of the age-matched controls (Figure 2): case 1, hypoperfusion in the frontal brain; case 2, no abnormal perfusion; and case 3, hypoperfusion in the frontal brain and cerebellum.[7] Magnetic resonance spectroscopic examinations were performed using a conventional whole-body system (Signa Horizon 1.5 Tesla, General Electric). Localization of a 20 × 20 × 20 mm region of interest in the right frontal lobe, occipital lobe, or basal ganglia was achieved using short echo time (30 milliseconds) point-resolved spectro-

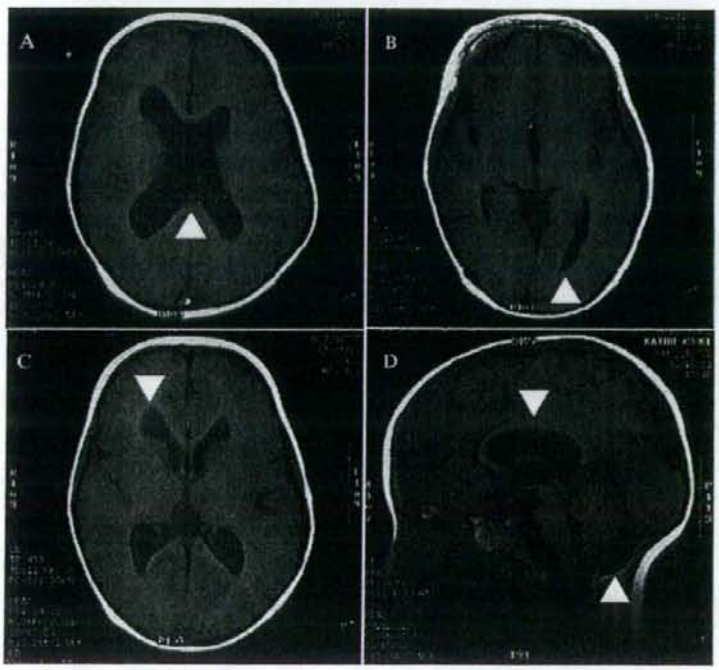

Figure 1. Magnetic resonance image (MRI) of the representative case (case 1). *A* to *C*, Axial sections of a T_1-weighted image; *D*, sagittal section of a T_1-weighted image. *Arrowheads* indicate abnormal lesions, which are typically observed in patients with Sotos syndrome (see Table 1).

Table 1. Magnetic Resonance Imaging Findings in Sotos Syndrome

Abnormalities	*Schaefer et al*[4]	*Case* 1	2	3
Ventricles				
Large	25/40	+	+	+
Prominent trigone	36/40	+	+	+
Prominent occipital horn	30/40	+	+	+
Extracerebral fluid				
Supratentorial	28/40	+	+	−
Posterior fossa	28/40	+	−	+
Midline anomalies				
Cavum septum pellucidum	16/40	−	−	+
Cavum vergae	15/40	−	−	+
Cavum velum interpositum	7/40	−	−	−
Macrocisterna magna	6/36	−	−	+
Agenesis of corpus callosum	1/40	−	−	−
Hypoplasia of corpus callosum	12/36	+	+	+
Thinning of corpus callosum body	23/36	−	−	−
Migrational				
Heterotopias	3/36	−	−	−
Others				
PVL	5/36	−	−	−
Macrocerebellum	2/36	−	−	−
Open operculum	1/40	−	−	−

PVL = periventricular leukomalacia; + = present; − = absent.

scopy sequences. The spectrum obtained from the frontal brain of the patients showed an increase in choline (3.22 ppm, choline to creatine ratio =1.15 in case 1, 1.20 in case 2, and 1.14 in case 3; age-matched controls: mean ± SD = 0.77 ± 0.05) resonances (Figure 3), whereas the spectrum obtained from the occipital brain or basal ganglia of the patients did not show any obvious increase in choline (choline to creatine = 0.74 in case 1, 0.87 in case 2, and 0.65 in case 3 for the occipital brain; 0.79 in case 1, 0.74 in case 2, and 0.79 in case 3 for the basal ganglia) resonances.

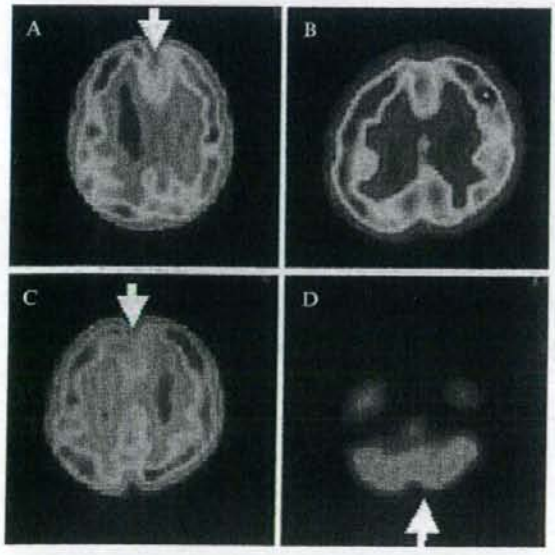

Figure 2. Single-photon emission computed tomography: axial sections of the brain show hypoperfusion of the frontal lobes. *Arrows* indicate the regions with abnormal intensity or perfusion. *A*, Case 1; *B*, case 2; *C* and *D*, case 3.

Discussion

The largest study by Schaefer et al reported that the neuroimaging anomalies frequently found in Sotos syndrome are large ventricles, increased extracerebral fluid, and midline anomalies.[4] All of our patients had similar abnormalities, at different degrees. These morphologic abnormalities of the brain should be associated with mental and motor retardation in patients with Sotos syndrome. The findings also suggests that a severity of the MRI abnormalities should correlate with a severity of developmental delay, but it requires a further precise study.

Two of the three patients here showed hypoperfusion in the frontal brain, whereas one patient showed hypoperfusion in the cerebellum (see Figure 2, A, C, and D), but there have been no reports about SPECT or positron emission tomographic findings in Sotos syndrome. Magnetic resonance spectroscopy in our patients also revealed abnormality in the frontal brain, not in the other regions, and high choline to creatine ratios. Choline to creatine ratios generally decrease with aging, and elevation in this ratio has been interpreted as a result of membrane degradation or as a result of choline synthesis associated with increased cellular proliferation being associated with brain maturity.[8] Flippi et al examined the magnetic resonance spectroscopic images of children with developmental delay or normal controls, and elevations in the choline to creatine ratios were detected in the frontal and parieto-occipital regions of the patients with developmental delay compared with age-matched control subjects.[9] The high choline to creatine ratios in our patients could be the result of the immaturity of the frontal lobe.

It has been reported that patients with Sotos syndrome have a significant tendency toward aggressiveness as a behavioral problem,[10–12] and two of our patients (cases 1 and 2) had significant aggressive behavior. The frontal brain has several important association areas, which control emotions. The immaturity of the frontal brain indicated here suggests that there are some associations with aggressive behavior in Sotos syndrome, but the observation is a preliminary one. Further studies, especially on the functional and psychologic aspects of Sotos syndrome, are required.

Hiroko Horikoshi, MD
Zenichiro Kato, MD
Department of Pediatrics
Graduate School of Medicine
Gifu University
Gifu, Japan

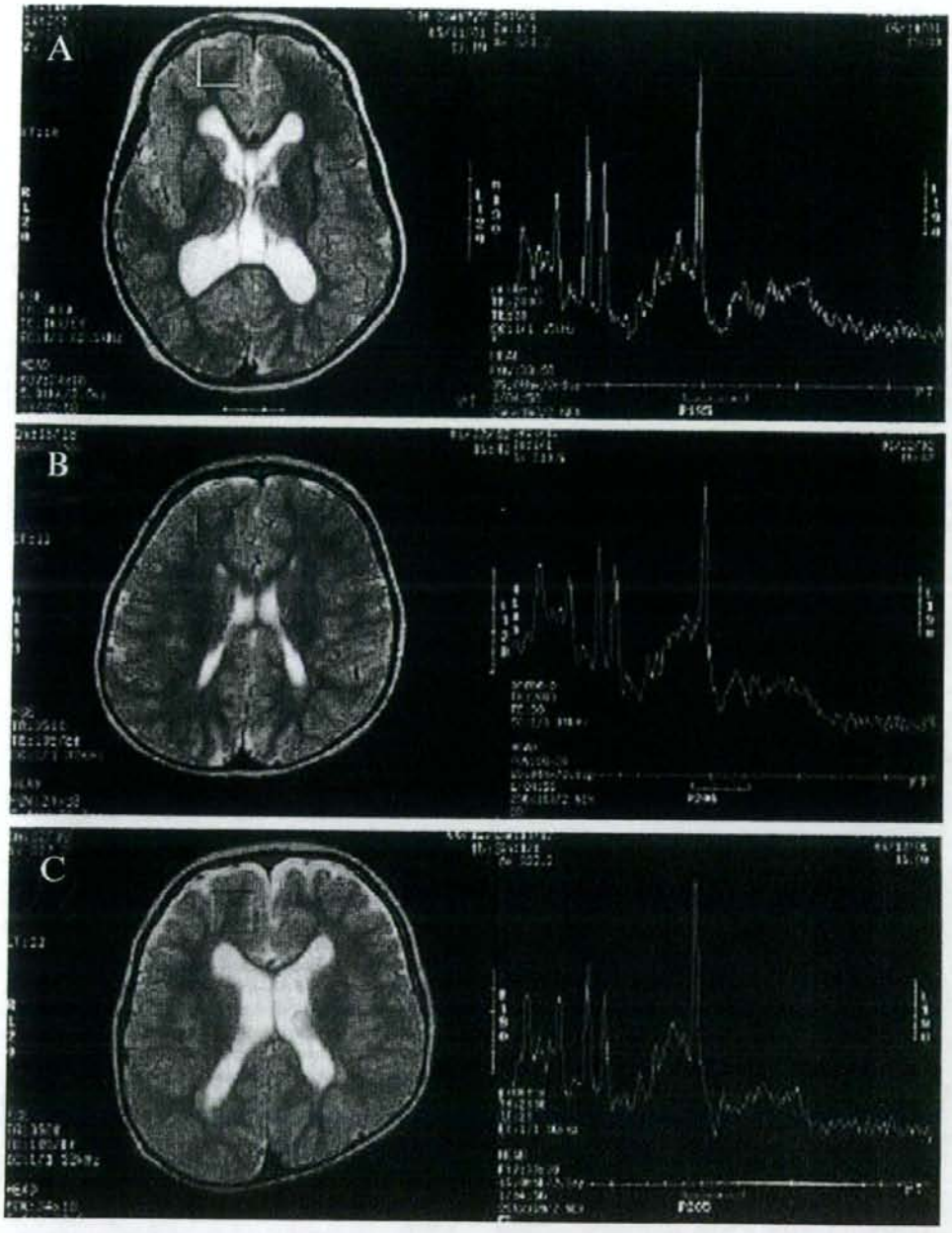

Figure 3. Magnetic resonance spectroscopy. Axial sections of T_2-weighted images and the spectrum obtained from the region of interest of the frontal lobe. *Squares* show the regions of interest in spectroscopic studies. *A*, Case 1; *B*, case 2; *C*, case 3.

Mitsuo Masuno, MD
Department of Pediatrics
Graduate School of Medicine
Gifu University
Gifu, Japan
Department of Nursing
Faculty of Health and Welfare
Kawasaki University of Medical Welfare
Kurashiki, Japan

Takahiko Asano, MD
Department of Radiology
Graduate School of Medicine
Gifu University
Gifu, Japan
Tomoko Nagase, MD
Yuka Yamagishi, MD
Ryo Kozawa, MD
Takahiro Arai, MD

Minako Aoki, MD
Takahide Teramoto, MD
Kentaro Omoya, MD
Department of Pediatrics
Graduate School of Medicine
Gifu University
Gifu, Japan
Naomichi Matsumoto, MD
Department of Human Genetics
Nagasaki University School of Medicine
Nagasaki, Japan
Department of Human Genetics
Yokohama City University Graduate School of Medicine
Yokohama, Japan
Naohiro Kurotaki, MD
Department of Human Genetics
Nagasaki University School of Medicine
Nagasaki, Japan
Department of Molecular and Human Genetics
Baylor College of Medicine
Houston, Texas
Osamu Shimokawa, MD
Department of Human Genetics
Nagasaki University School of Medicine
Nagasaki, Japan
Kyushu Medical Science Nagasaki Laboratory
Nagasaki, Japan
Kenji Kurosawa, MD
Division of Medical Genetics
Kanagawa Children's Medical Center
Yokohama, Japan
Naomi Kondo, MD
Department of Pediatrics
Graduate School of Medicine
Gifu University
Gifu, Japan

Received March 16, 2005. Received revised May 25, 2005. Accepted for publication July 26, 2005

Address correspondence to Dr Zenichiro Kato, Department of Pediatrics, Graduate School of Medicine, Gifu University, Yanagido 1-1, Gifu 501-1194, Japan. Tel: +81 (58) 230 6386; fax: +81 (58) 230 6387; e-mail: zen-k@cc.gifu-u.ac.jp.

References

1. Sotos JF, Dofge PR, Muirhead D, et al: Cerebral gigantism in childhood. *N Engl J Med* 1964;271:109–116.
2. Cole TRP, Hughes HE: Sotos syndrome: A study of the diagnostic criteria and natural history. *J Med Genet* 1994;31:20–32.
3. Kurotaki N, Imaizumi K, Harada N, et al: Haploinsufficiency of NSD1 causes Sotos syndrome. *Nat Genet* 2002;30:365–366.
4. Schaefer GB, Bodensteiner JB, Buehler BA, et al: The neuroimaging findings in Sotos syndrome. *Am J Med Genet* 1997;68:462–465.
5. Aoki N, Oikawa A, Sakai T: Serial neuroimaging studies in Sotos syndrome. *Neurol Res* 1998;20:149–152.
6. Inoue K, Kato S, Numaga J, et al: Optic disk pallor and retinal atrophy in Sotos syndrome. *Am J Ophthalmol* 2000;130:853–854.
7. Mizuno S, Nandate Y, Enya M, et al: Evalutaion of regional cerebral blood flow changes in normal aging using 99m-Tc-ECD SPECT and Patlak method. *Radioisotopes* 1998;47:392–398.
8. Danielsen ER, Ross B: *Magnetic Resonance Spectroscopy Diagnosis of Neurological Diseases*, 3rd ed. New York, Marcel Dekker, 1999.
9. Flippi CG, Ulug AM, Deck MD, et al: Developmental delay in children: Assessment with proton MR spectroscopy. *AJNR Am J Neuroradiol* 2002;23:882–888.
10. Rutter SC, Cole TR: Psychological characteristics of Sotos syndrome. *Dev Med Child Neurol* 1991;33:898–902.
11. Finegan JK, Cole TR, Kingwell E, et al: Language and behavior in children with Sotos syndrome. *J Am Acad Child Adolesc Psychiatry* 1994;33:1307–1315.
12. Mauceri L, Sorge G, Baieli S, et al: Aggressive behavior in patients with Sotos syndrome. *Pediatr Neurol* 2000;22:64–67.

American Journal of Medical Genetics Part A 143A:98–101 (2007)

Research Letter

Angelman Syndrome Caused by an Identical Familial 1,487-kb Deletion

Kanako Sato,[1] Mie Iwakoshi,[2] Osamu Shimokawa,[3,4] Haruya Sakai,[1] Tohru Ohta,[5] Shinji Saitoh,[6] Noriko Miyake,[4] Norio Niikawa,[4] Naoki Harada,[3] Hirotomo Saitsu,[1] Takeshi Mizuguchi,[1] and Naomichi Matsumoto[1]*

[1]Department of Human Genetics, Yokohama City University Graduate School of Medicine, Yokohama, Japan
[2]Nishinomiya Municipal Wakaba-en, Nishinomiya, Japan
[3]Kyushu Medical Science Nagasaki Laboratory, Nagasaki, Japan
[4]Departments of Human Genetics, Nagasaki University Graduate School of Biomedical Sciences, Nagasaki, Japan
[5]The Research Institute of Personalized Health Sciences, Health Sciences University of Hokkaido, Ishikari-tobetsu, Japan
[6]Department of Pediatrics, Hokkaido University School of Medicine, Sapporo, Japan

Received 25 August 2006; Accepted 29 September 2006

How to cite this article: Sato K, Iwakoshi M, Shimokawa O, Sakai H, Ohta T, Saitoh S, Miyake N, Niikawa N, Harada N, Saitsu H, Mizuguchi T, Matsumoto N. 2007. Angelman syndrome caused by an identical familial 1,487-kb deletion. Am J Med Genet Part A 143A:98–101.

To the Editor:

Angelman syndrome (AS, OMIM #105830) is a neurodevelopmental disorder characterized by mental retardation, ataxia, hypotonia, epilepsy, absence of speech, and specific facial features. At least four major mechanisms causing AS were validated: (i) an interstitial deletion of 15q11-q13 (70–75%), (ii) uniparental disomy (2–3%), (iii) imprinting defects (3–5%), (iv) *UBE3A* mutations (20%) [Clayton-Smith and Laan, 2003]. Most deletions are similar in size (approximate 4 Mb) and occur de novo through maternal unequal crossing over between low copy repeats (LCRs). Paternal occurrence of similar deletions, instead, results in Prader–Willi syndrome (PWS, OMIM #176270). In PWS no coding mutations have been found in contrast with *UBE3A* mutations in AS, suggesting that PWS is caused by loss of function of multiple genes.

Different sized deletions associated with AS are very rare. To our knowledge, at least three familial atypical deletions were reported [Saitoh et al., 1992; Buxton et al., 1994; Burger et al., 2002], but in one family [Buxton et al., 1994] a microdeletion could not be confirmed by another group [Sutcliffe et al., 1997]. In the remaining two families, microdeletions caused AS in maternal inheritance but no PWS features in paternal inheritance, enabling differentiation of the PWS critical region (PWSCR) from the AS critical region (ASCR).

We encountered a similar family with an atypical microdeletion through microarray CGH analysis of 30 individuals with idiopathic mental retardation [Miyake et al., 2006]. The family consisted of a boy, who was later confirmed with AS, and an asymptomatic mother and maternal grandfather (Fig. 1A). All three had an atypical microdeletion. Methylation PCR analysis [Kubota et al., 1997] of the proband showed a normal pattern (data not shown).

The deletion was intensively analyzed. FISH analysis using RPCI-11 BAC clones (701H24, 171C8, 1081A4, 607F22, 931B1, 2C7, 434O21, 203C13, 638J6, 899B22, 58D7, and 142M24) on the proband's metaphase chromosomes revealed that 1081A4, 607F22, 931B1, 2C7, 434O21, 203C13, 638J6, 899B22, and 58D7 were deleted, 171C8 and 142M24 were partially deleted, and 701H24 was not deleted (data not shown). Cosmid subclones constructed from BAC 171C8 were used for further FISH analysis. Cosmid D-2 was partially deleted (data not shown), indicating that the proximal deletion breakpoint was located in a region between UCSC coordinate chromosome 15 nucleotide 22,928,853 and 22,974,812 (end sequences of cosmid D-2). Subsequently quantitative real-time PCR (qPCR)

Grant sponsor: Ministry of Health, Labour and Welfare; Grant sponsor: Yokohama Foundation for Advancement of Medical Science; Grant sponsor: Mitsubishi Foundation; Grant sponsor: SORST, Japan Science and Technology Agency (JST).

*Correspondence to: Naomichi Matsumoto, Department of Human Genetics, Yokohama City University Graduate School of Medicine, Fukuura 3-9, Kanazawa-ku, Yokohama 236-0004, Japan.
E-mail: naomat@yokohama-cu.ac.jp

DOI 10.1002/ajmg.a.31550

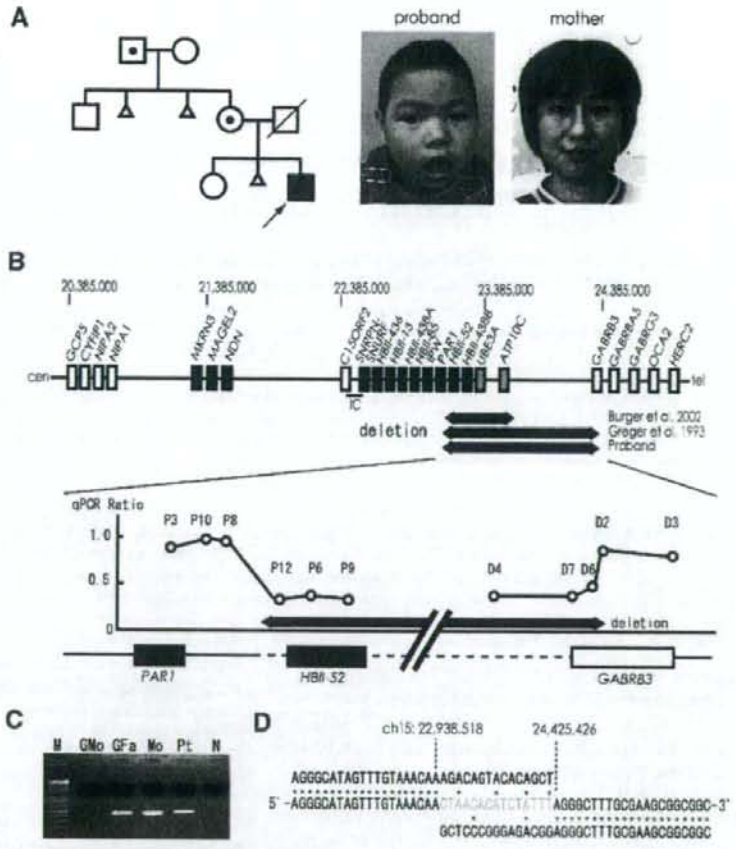

FIG. 1. **A**: Pedigree of the family and photographs of the proband (arrow) and his mother. Proband, mother, and maternal grandfather (dotted) had a deletion. His father died of biliary atresia at 31 years old. **B**: Schematic presentation of genes (black boxes: genes expressed from paternal chromosome, gray boxes: genes expressed from maternal chromosome, open boxes: genes expressed from both chromosomes), rare familial deletions, and result of quantitative real-time PCR (qPCR) analysis. Deletion from *HBII-52* cluster to *GABRB3* was confirmed. **C**: Deletion specific PCR analysis of the family. PCR using primers, DSF and DSR, could successfully amplify a 2.6-kb product from grandfather (GFa), mother (Mo), and patient (Pt), but not from grandmother (GMo). M: size marker, N: negative control. **D**: Sequence of deletion breakpoints. The sequence in a middle row indicates the patient's sequence spanning the deletion. Upper and lower rows show normal sequences corresponding to centromeric and telomeric to the deletion. Proximal and distal deletion breakpoints are marked with UCSC coordinate chromosome 15 nucleotide positions. Fifteen nucleotides (in gray) were inserted. Asterisks indicate nucleotides identical to normal chromosome 15 sequence.

using DyNAmo HS SYBR Green qPCR kit (Finnzymes, Espoo, Finland) was conducted to determine breakpoint locations according to the methods by Boehm et al. [2004] with some modification. A total of six sets of primers (P3, P10, P8, P12, P6, and P9) as test probes were designed within the cosmid D-2 region along with a control primer set for *FBN1* locus at 15q21.1. Rotor-Gene™ 6200 HRM (Corbett Life Science, Sydney, Australia) could demonstrate a heterozygous deletion for primer-sets P12, P6, and P9 (Fig. 1B). Similarly five sets of primers (D4, D7, D6, D2, and D5) were selected from the region of BAC 142M24 and three sets, D4, D7, and D6, implied a deletion. Thus proximal and distal deletion breakpoints seemed to exist between P8 and P12 and between D6 and D2, respectively. Finally deletion breakpoints were successfully amplified as an approximate 2.6-kb product by PCR using LA-Taq (Takara Bio Inc., Otsu, Japan) and primers (DSF: 5′-TATAACTAGGTATTGGACTCATACTGAGGA-3′ and DSR: 5′-ACCTACAGCCTTCTAAGTACTGTATCCAT-3′) from the patient's DNA as well as his mother and maternal grandfather, but not from his maternal grandmother (Fig. 1C) or 10 normal controls. The PCR products were sequenced (Fig. 1D). The proband, his mother, and maternal grandfather had exactly the same breakpoint sequences. The deletion was 1,487-kb in size and